

UC San Diego

UC San Diego Previously Published Works

Title

Reproducible sequence generation in random neural ensembles

Permalink

<https://escholarship.org/uc/item/7wf8d0sq>

Journal

Physical Review Letters, 93(23)

ISSN

0031-9007

Authors

Huerta, Ramon

Rabinovich, M

Publication Date

2004-12-01

Peer reviewed

Reproducible Sequence Generation In Random Neural Ensembles

Ramón Huerta* and Mikhail Rabinovich

Institute for Nonlinear Science, University of California, San Diego, La Jolla, California 92093-0402[†], USA
(Received 24 February 2004; published 2 December 2004)

Little is known about the conditions that neural circuits have to satisfy to generate reproducible sequences. Evidently, the genetic code cannot control all the details of the complex circuits in the brain. In this Letter, we give the conditions on the connectivity degree that lead to reproducible and robust sequences in a neural population of randomly coupled excitatory and inhibitory neurons. In contrast to the traditional theoretical view we show that the sequences do not need to be learned. In the framework proposed here just the averaged characteristics of the random circuits have to be under genetic control. We found that rhythmic sequences can be generated if random networks are in the vicinity of an excitatory-inhibitory synaptic balance. Reproducible transient sequences, on the other hand, are found far from a synaptic balance.

DOI: 10.1103/PhysRevLett.93.238104

PACS numbers: 87.18.Sn, 05.45.-a, 87.18.Bb, 89.75.Hc

Introduction.—At the behavioral level, to be successful an animal not only has to learn a specific task, it also needs to learn specific sequences or orders of tasks. At the neural level, reproducible sequential neural activity has been shown to be crucial in a variety of cases, such as processing of sensory information [1], animal communication [2], and motor control and coordination [3]. All these intriguing experimental observations pose the problem about how to generate reproducible and robust sequences of neural activity. Our working hypothesis is that neural systems that generate sequences carry out just this task: To create stimulus dependent reproducible sequences (RS) that are robust against perturbations. As shown in [4], a learning phase for a specific computational task can be efficiently carried out at later stages. Our main goal is to determine the design conditions for the neural system generating sequential activity that leads to robust RS. We here want to investigate how these RS can emerge spontaneously without any learning rule or external guidance. The basic network in our investigation is a Bernoulli random graph. This is the simplest network of excitatory and inhibitory neural clusters because it only requires a few control parameters: probabilities of making a connection from one cluster type to another. Thus, nature just needs to encode the probability of connections in the genetic code to realize such a network. If we can find parameter values for which it is very likely to find RS, then we can argue that random networks are a suitable substrate for RS generation in the nervous system.

In this Letter, we determine that the area of the highest likelihood to find limit cycles is slightly shifted with respect to the one that provides balanced excitatory-inhibitory synaptic input to each cluster of neurons. On the other hand, regarding transient behavior, RS are found far from the region of balanced excitatory-inhibitory synaptic input. This dichotomy poses the fundamental question about what alternative sensory systems may choose. A strong argument is that sensory systems react

as fast as possible to exogenous perturbations or stimuli. It is, therefore, very likely that neural systems responsible for sequence generation use transient dynamics and, thus, they are not located near the region of balanced excitatory-inhibitory synaptic connectivity.

Model.—We analyze a Wilson-Cowan type network of excitatory and inhibitory clusters of neurons [5], whose simplified ordinary differential equations (ODE) are given by

$$\frac{1}{\beta} \frac{dx_i}{dt} = \Theta \left(\sum_{j=1}^{N_E} w_{ij}^{EE} x_j - \sum_{j=1}^{N_I} w_{ij}^{EI} y_j + S_i^E \right) - x_i, \quad (1)$$

$$\frac{1}{\beta} \frac{dy_i}{dt} = \Theta \left(\sum_{j=1}^{N_E} w_{ij}^{IE} x_j - \sum_{j=1}^{N_I} w_{ij}^{II} y_j + S_i^I \right) - y_i, \quad (2)$$

where x_i and y_i represent the fraction of active neurons in cluster i of the excitatory and inhibitory population, respectively, and the numbers of excitatory and inhibitory clusters are N_E and N_I . Throughout this Letter E is used to denote a quantity of the excitatory population and I to denote those of the inhibitory population. The external inputs $S_{E,I}$ are instantaneous “kicks” at time zero applied to a fraction of the total population. The gain function is $\Theta(z) = \frac{1}{2} [\tanh((z - b)/\sigma) + 1]$, with a threshold $b = 0.1$ below the excitatory and inhibitory synaptic strength of a single connection. We will assume that the clusters have very sharp excitability, such that in all the simulations we set $\sigma = 0.01$. Nevertheless, there is a wide range of σ values that generates similar results. The simulations deviate from the theoretical estimations for $\sigma \geq 0.5$. The time scale is set as in [5], $\beta^{-1} = 10$ ms. The connectivity matrices, w_{ij}^{XY} , have entries drawn from the following Bernoulli process

$$w_{ij}^{XY} = g^Y \begin{cases} 1 & \text{with probability } p_{XY}, \\ 0 & \text{otherwise.} \end{cases} \quad (3)$$

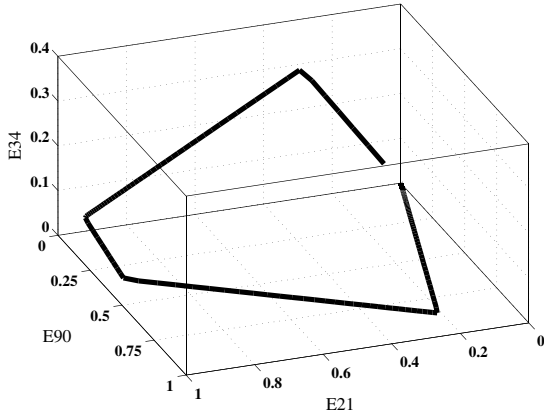


FIG. 1. Phase portrait of RS of three clusters using $p_{EE} = 0.05$, $p_{EI} = 0.3$, $p_{IE} = 0.1$, $p_{II} = 0.15$, and $g^E = 2$, $g^I = 0.2$ with $N_E = N_I = 100$.

where $X, Y = E, I$. An example of RS by the Wilson-Cowan model is shown in Fig. 1.

Methods.—To detect limit cycles we used a simple algorithm that stores the order in which neuron clusters pass a certain threshold value in an array. We fixed this threshold exactly at the average value of the total activity. In the list of active clusters we detect repetitions of sequences of active clusters. This method for limit cycle detection is fast to compute but it can underestimate the number of limit cycles because there can be oscillations at higher or lower levels than the chosen threshold.

To detect the degree of reproducibility during transient dynamics we build a graph where each node represents a cluster label i and each edge is the probability to go from one cluster to the next, $p_{i \rightarrow j}$. This graph with its transition probabilities is built using the statistics gathered from runs with 50 different initial conditions. We then calculate the entropy of the outdegree edges belonging to each node, $S_i = -\sum_j p_{i \rightarrow j} \log p_{i \rightarrow j}$. If the sequence of activity is highly reproducible then $S_i = 0$. If the transition from one cluster to the next is uniformly random then $S_i = \log N_E$. We build the graph only with the excitatory population because it is the driving force in our model. As a measure of reproducibility we then use $S = (1/N_E) \sum_i S_i$.

Probability map.—In parallel to the numerical work we build statistical estimators that predict the activity of the excitatory and inhibitory populations. This activity estimation allows us to determine the region where we can expect a maximal probability of crossing the threshold, where balanced excitation and inhibition exists [6], and where to expect better chances of having reproducible sequences. To build our estimators we make the assumption of homogeneity and statistical independence between the state of the system and the network connectivity. This second assumption is widely used to build estimators of measures over random network dynamics [7,8].

To avoid solving a partial differential equation for the probability distributions, we assume that the states of the

clusters are either one or zero; that gives us good approximations for $\sigma \leq 0.5$. Then, we assign a constant transition probability μ to jump from one state to the other at each time step. When starting with 1 (0), the probability to still be 1 (0) after n iterations is proportional to $\exp(-\mu n)$. On the other hand, if we integrate the ODEs for a single cluster its value either decays or grows as $\exp(-\beta t)$. Therefore, we match the stochastic to the deterministic process by setting $\mu n = \beta t$.

Let us define x and y as the homogeneous variables representing the state of the excitatory and inhibitory population. We want to calculate the probability of the state $x(t), y(t)$ at time t given the state at time $t - 1$. In order to do so we define the following events: the event \mathcal{A}_X and \mathcal{A}_Y when the clusters receive a level of depolarization higher than or equal to the threshold, i.e., $\mathcal{A}_X \equiv \sum_{j=1}^{N_E} w_{ij}^{EE} x_j - \sum_{j=1}^{N_I} w_{ij}^{EI} y_j \geq b$ and $\mathcal{A}_Y \equiv \sum_{j=1}^{N_E} w_{ij}^{IE} x_j - \sum_{j=1}^{N_I} w_{ij}^{II} y_j \geq b$. Whenever these events are not present at a given time, the dynamics is reduced to just the decay process. An estimate for the probability of having the event \mathcal{A}_X given some activity levels of the excitatory and inhibitory populations is

$$p_{t-1}(\mathcal{A}_X | e, i) = \sum_{\forall (c_E, c_I) | c_E g_{EE} - c_I g_{EI} \geq b} b_{e, p_{EE}}(c_E) b_{i, p_{EI}}(c_I),$$

where $b_{e, p_{EE}}(c_E)$ and $b_{i, p_{EI}}(c_I)$ are binomial distributions, $b_{Np}(c) = \binom{N}{c} p^c (1-p)^{N-c}$, with e and i the number of active excitatory and inhibitory clusters and c representing the number of coactive clusters and connections. We can only count the synaptic contribution if an active cluster has a connection to another cluster. p_{EE} , p_{EI} , p_{IE} , and p_{II} are the probabilities of connections from population to population as described earlier. Similarly,

$$p_{t-1}(\mathcal{A}_Y | e, i) = \sum_{\forall (c_E, c_I) | c_E g_{IE} - c_I g_{II} \geq b} b_{e, p_{IE}}(c_E) b_{i, p_{II}}(c_I).$$

Then, we calculate

$$p_{t-1}(\mathcal{A}_X) = \sum_{\forall e, i} p_{t-1}(\mathcal{A}_X | e, i) p_{t-1}(e) p_{t-1}(i),$$

$$p_{t-1}(\mathcal{A}_Y) = \sum_{\forall e, i} p_{t-1}(\mathcal{A}_Y | e, i) p_{t-1}(e) p_{t-1}(i),$$

where $p_{t-1}(e) = b_{N_E p_{t-1}(x=1)}(e)$ and $p_{t-1}(i) = b_{N_I p_{t-1}(y=1)}(i)$. This assumes that the probability distribution of the activity levels is unimodal and very close to a binomial distribution [9]. We then solve $p_t(x=1) = p_{t-1}(x=1 | \mathcal{A}_X, x=0) p_{t-1}(\mathcal{A}_X) p_{t-1}(x=0) + p_{t-1}(x=1 | \mathcal{A}_X, x=1) p_{t-1}(\mathcal{A}_X) p_{t-1}(x=1) + p_{t-1}(x=1 | \overline{\mathcal{A}}_X, x=0) p_{t-1}(\overline{\mathcal{A}}_X) p_{t-1}(x=0) + p_{t-1}(x=1 | \overline{\mathcal{A}}_X, x=1) p_{t-1}(\overline{\mathcal{A}}_X) p_{t-1}(x=1)$ (with a similar expression for $p_t(y=1)$) to obtain the following dynamical map:

$$p_t(x=1) = \mu p_{t-1}(\mathcal{A}_X) + (1-\mu) p_{t-1}(x=1), \quad (4)$$

$$p_i(y=1) = \mu p_{i-1}(\mathcal{A}_Y) + (1-\mu)p_{i-1}(y=1). \quad (5)$$

The smaller μ the better is the equivalence between the deterministic and stochastic equations. A value of $\mu = 0.1$ seems to be a good compromise between computing time and proximity to the deterministic system. Figure 2 shows the similarities of the model with the simulations for 2000 different random graphs. The average activity of the excitatory population is $\nu_E = \langle (1/N_E) \sum_i \langle x_i(t) \rangle_{t=\tau..T} \rangle_G$ and the inhibitory one is $\nu_I = \langle (1/N_I) \sum_i \langle y_i(t) \rangle_{t=\tau..T} \rangle_G$, where G represents the set of graphs generated by Eq. (3) which do not lead to the absorbing state. τ is the offset to start recording after some transient and T is chosen to average several cycles.

The main driving force of the system is the excitatory population because of the short initial pulse. There must be sufficient excitation to sustain the activity of the network but not too much activity because the network otherwise reaches its saturation level. To reduce our search of the parameter space we use the estimation for the activity given by Eqs. (4) and (5), to search the curve of balanced synaptic input [6]. We also look at the maximum probability of crossing the threshold, inspired by the ideas of [10] for boolean networks, and, in addition, we estimate the probability of having reproducible sequences. First, the curve of balanced synaptic input is estimated from the implicit equation $N_E \nu_E(p_{EE}, p_{EI}, p_{IE}, p_{II}) g_E p_{EE} - N_I \nu_I(p_{EE}, p_{EI}, p_{IE}, p_{II}) g_I p_{EI} = b$, which is the total expected synaptic input into a given excitatory cluster. Second, to estimate the curve where the probability of crossing the threshold is maximal, we use $h = p_{i-1}(x=1|x=0)p_{i-1}(x=0) + p_{i-1}(x=0|x=1)p_{i-1}(x=1)$, where, for example, $p_{i-1}(x=1|x=0) = p_{i-1}(x=1|\mathcal{A}_X, x=0)p_{i-1}(\mathcal{A}_X) + p_{i-1}(x=1|\overline{\mathcal{A}}_X, x=0)p_{i-1}(\overline{\mathcal{A}}_X) = \mu p_{i-1}(\mathcal{A}_X)$. Expanding the probability h as a function of the previous equations we obtain $h = \mu[p_{i-1}(\mathcal{A}_X)(1 - p_{i-1}(x=1)) + (1 - p_{i-1}(\mathcal{A}_X))p_{i-1}(x=$

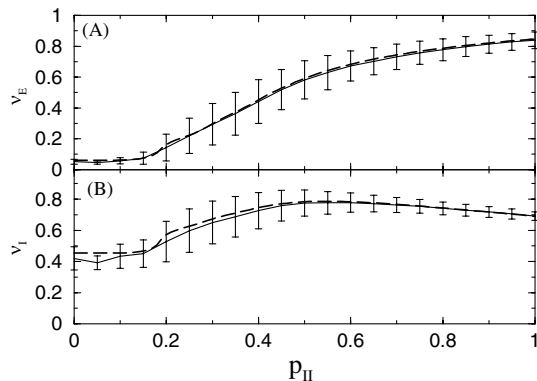


FIG. 2. Comparison between the simulations (solid lines with error bars) and the theoretical estimation (dotted line) for the excitatory (a) and inhibitory populations (b) obtained by using $p_{EE} = 0.05$, $p_{EI} = 0.3$, $p_{IE} = 0.1$, and $g^E = 2$, $g^I = 0.2$ with $N_E = N_I = 100$.

1)]. Third, to estimate the probability of having reproducible sequences we calculate the probability that two clusters end up in the same state. In other words, $r = \sum_{s_1, s_2} [p_{i-1}(x_1=1, x_2=1|x_1=s_1, x_2=s_2) + p_{i-1}(x_1=0, x_2=0|x_1=s_1, x_2=s_2)]p_{i-1}(x_1=s_1, x_2=s_2)$. To be able to estimate this we assume that the two clusters under consideration are statistically independent. We then expand on the events \mathcal{A}_X and $\overline{\mathcal{A}}_X$ as shown above to obtain a similar expression to h .

Results.—As pointed out in boolean networks [11] we also observe in our simulations that limit cycles involve a small number of clusters bounded by a frozen component. The region where these limit cycles are found is indicated in Fig. 3(a). The solid lines represent the curves of p_{EE} as a function of p_{II} solved for the implicit equation of the balance condition. For the parameter values indicated in Fig. 3 we find a small corridor from $p_{EE} = 0.02$ to $p_{EE} = 0.06$ where RS is found in the simulations. The dashed lines represent the probability of crossing the threshold h . We can see the maximum of h is always slightly shifted to the right from the curve corresponding to balanced synaptic input. Moreover, the theoretical curves converge into one single straight line for increasing values of p_{IE} . This

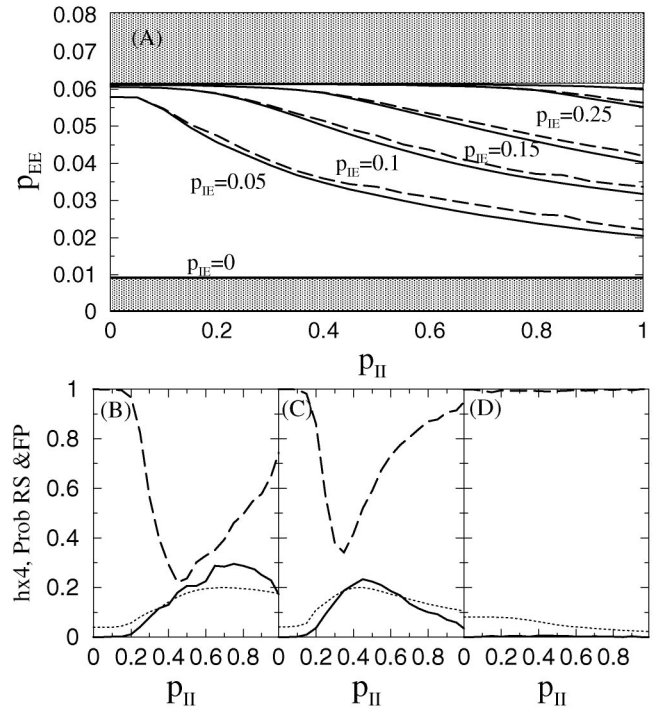


FIG. 3. (a) Estimation of the curve of balanced synaptic input (solid line) and maximum probability of crossing the threshold. The parameter values of this figure are $p_{EI} = 0.3$ and $g^E = 2$, $g^I = 0.2$ with $N_E = N_I = 100$ for $p_{IE} = 0.0, 0.05, 0.1, 0.2, 0.3, 0.4$. (b-d) Result of simulations of the limit cycle (solid lines) and fixed points (dashed lines) with parameter values for (b) $p_{EE} = 0.04$, (c) $p_{EE} = 0.05$, and (d) $p_{EE} = 0.07$. We also compare them to the probability of crossing the threshold, h , which is the dotted line.

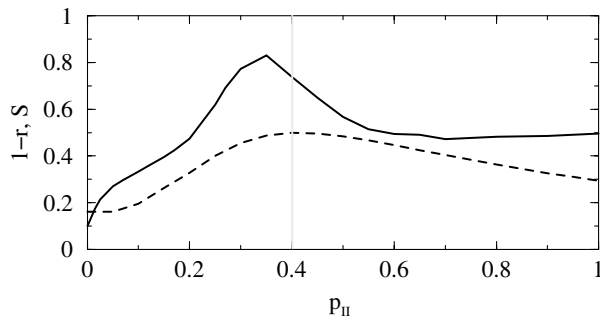


FIG. 4. Entropy measure (solid line) of the reproducibility of the sequential activity for parameter values $p_{EE} = 0.05$ as in Fig. 3. The dashed line represents the estimation of falling into different states, $1 - r$.

limiting line is the boundary of an area (gray patterned area) where RS cannot be obtained. This is due to the excessive amount of excitation in the system that drives it into saturation levels. Figures 3(b)–3(d) show the results of the simulations after the transients. The maximal probability for finding limit cycles is observed at the maximum of the probability of crossing the threshold h . Comparing to Fig. 3(a) we can see that for $p_{EE} = 0.07$ (the gray area) no limit cycles exist. Comparing the simulations shown in Fig. 3(b) and 3(c) the minimum number of fixed points is found on the left of the theoretical lines. Therefore, the theoretical lines bound the region where RS can be found and h can pinpoint the location of maximal limit cycle occurrence.

Sensory systems are known to respond fast to external stimuli. Thus, we want to determine the locations of RS during transient dynamics. We also want to compare the parameter values to those ones obtained by the balanced network conditions. Figure 4 shows the entropy measure as defined earlier as a function of p_{II} for the same parameter values as in Fig. 3(c). The worst reproducibility values are observed near the condition of balanced excitation and inhibition. The main reason is that in this area we find chaotic behavior and the smallest percentage of fixed points. The left region of the balanced network displays a large percentage of fixed points. Therefore, it is not surprising to find better reproducibility. The right hand side of the balanced network condition shows a plateau of reproducibility also due to the fast increase of fixed point percentage. The estimation of reproducibility r disregards any correlations between clusters, nevertheless it gives a qualitative indication of where it is more likely to find RS.

Conclusion.—Because even the simplest part of a brain is an extremely complex system in terms of the number of

neurons and, mainly, synapses, and the variability of connections, a simple estimation shows that is not possible to specify the network connectivity in the genome. We showed that just a few parameters need to be controlled by the genetic code to be able to generate RS. We showed that reproducible transient dynamics is appropriate for sequence generation if the network is far from having balanced synaptic input. The dynamical mechanisms underlying the generation of sequences need a more detailed analysis. However, the similarity of the random network data with sequences generated by complex circuits governed by the winnerless competition (WLC) principle [12] might lead us to believe that WLC is a mechanism responsible for both rhythmic and transient RS in random networks.

We want to thank Thomas Nowotny and Gabriel Mindlin for helpful discussions. This work was supported by Grant Nos. NSF/EIA-0130708 and NIH-1-R01-NS50945.

*Also at GNB, E.T.S. de Ingeniería Informática, Universidad Autónoma de Madrid, 28049 Madrid (Spain). Electronic address: rhuerta@ucsd.edu.

†URL: <http://inls.ucsd.edu/>

- [1] G. Laurent *et al.* *Annu. Rev. Neurosci.* **24**, 263 (2001).
- [2] R. H. R. Hahnloser *et al.*, *Nature (London)* **419** 65 (2002).
- [3] A. Selverston, *Prog. Brain Res.* **123**, 247 (1999); O. Melamed *et al.* *Trends Neurosci.* **27**, 11 (2004); J.W. Aldridge and K. C. Berridge *J. Neurosci.* **18**, 2777 (1998).
- [4] W. Maass *et al.* *Neural Comput.* **14**, 2531 (2002); H. Jaeger and H. Haas, *Science* **304**, 78 (2004).
- [5] H. R. Wilson and J. D. Cowan, *Kybernetik* **13**, 55 (1973). In the model we analyze here we set the refractory periods to 0. Therefore, the rising and decay time constants of the model are identical.
- [6] C. van Vreeswijk and H. Sompolinsky, *Neural Comput.* **10**, 1321 (1988).
- [7] N. Bertschinger and T. Natschlager, *Neural Comput.* **16**, 1413 (2004).
- [8] B. Derrida and Y Pomeau, *Europhys. Lett.* **1**, 45 (1986).
- [9] The activity distribution is actually bimodal because there is always a peak in the absorbing state. The results that we analyze in the simulations are obtained without counting the absorbing states.
- [10] L. Glass, *J. Chem. Phys.* **63**, 1325 (1975); L. Glass and J. Pasternack, *J. Math. Biol.* **6**, 207 (1978).
- [11] S. A. Kauffman, *The Origins of Order: Self-Organization in Evolution* (Oxford University Press, New York, 1993).
- [12] M. Rabinovich *et al.* *Phys. Rev. Lett.*, **87**, 068102 (2001).